

THE FIRST MEASUREMENTS OF THE ELECTRON DENSITY ENHANCEMENTS EXPECTED IN C-TYPE SHOCKS

I. JIMÉNEZ-SERRA,¹ J. MARTÍN-PINTADO,¹ S. VITI,² S. MARTÍN,³ A. RODRÍGUEZ-FRANCO,^{1,4} A. FAURE,⁵ AND J. TENNYSON²

Received 2006 July 11; accepted 2006 September 6; published 2006 October 4

ABSTRACT

Magnetic precursors of C-type shocks accelerate, compress, and heat molecular ions, modifying the kinematics and the physical conditions of the ion fluid with respect to the neutral one. Electron densities are also expected to be significantly enhanced in shock precursors. In this Letter, we present observations of strongly polar ion and neutral molecules such as SiO, H¹³CO⁺, HN¹³C, and H¹³CN, which reveal the electron density enhancements associated with the precursor of the young L1448-mm outflow. While in the ambient gas the excitation of the ions and neutrals is explained by collisional excitation by H₂ with a single density of $\sim 10^5$ cm⁻³, H¹³CO⁺ shows an overexcitation in the shock precursor component that requires H₂ densities a factor of ≥ 10 larger than those derived from the neutral species. This overexcitation in H¹³CO⁺ can be explained if we consider an additional excitation by collisions with electrons and an electron density enhancement in the precursor stage by a factor of ~ 500 , i.e., a fractional ionization of 5×10^{-5} . These results show that multiline observations can be used to study the evolution of the ion and electron fluids at the first stages of the C-type shock interaction.

Subject headings: ISM: individual (L1448) — ISM: jets and outflows — ISM: molecules — stars: formation

1. INTRODUCTION

In dense molecular clouds, the fractional ionization of the gas is very low ($\leq 10^{-7}$; Guélin et al. 1982; Caselli et al. 1998). Electron densities are therefore insufficient to excite the first rotational levels of even strongly polar molecules like HCO⁺, HCN, or HNC whose collisional cross sections ($\sim 10^{-6}$ to 10^{-5} cm³ s⁻¹; Bhattacharyya et al. 1981; Saha et al. 1981; Faure & Tennyson 2001) are a factor of ≥ 100 larger than those of weakly polar species like CO ($\sim 10^{-8}$ cm³ s⁻¹; Saha et al. 1981). All attempts to use molecular excitation to measure the effects of collisional excitation by electrons in these regions have been so far unsuccessful (Langer 1985).

Modeling of the early stages of C-type shocks predicts that the ion and electron densities are enhanced by the magnetic precursor (Draine 1980). For molecules like HCO⁺, HCN, or HNC, the electron density enhancement by a factor of ~ 100 produced by the precursor (see, e.g., Flower et al. 1996) would make electron collisions competitive with excitation by H₂ collisions for the typical densities of dark clouds ($\sim 10^5$ cm⁻³). Since the electron collisional coefficients for high initial J transitions of HCO⁺ are a factor of ≥ 10 larger than those of neutral molecules like HCN at low temperatures (~ 10 – 20 K; Chu & Dalgarno 1974; Bhattacharyya et al. 1981), differences in the molecular excitation between ion and neutral species are therefore expected in the precursor stage.⁶ Toward the young L1448-mm molecular outflow, the detection of very narrow SiO emis-

sion and the enhancement of the ion abundance have been interpreted as signatures of the shock precursor (Jiménez-Serra et al. 2004). Multiline observations of strongly polar species like HCO⁺, HNC, and HCN toward this outflow are expected to show differences in excitation between the ambient gas, where electron excitation is negligible, and the shock precursor, where electron collisions should be important.

In this Letter, we present observations of several rotational transitions of SiO, H¹³CO⁺, HN¹³C, and H¹³CN toward the ambient and shock precursor components of the L1448-mm outflow. The excitation differences observed between H¹³CO⁺ and SiO, HN¹³C, and H¹³CN in the ambient and precursor components can be explained by the electron density enhancement expected at the first stages of the C-type shock evolution.

2. OBSERVATIONS AND RESULTS

We observed several transitions (from $J = 1$ to 5) of SiO, H¹³CO⁺, HN¹³C, and H¹³CN toward three different positions in the L1448-mm outflow. Except for the $J = 4 \rightarrow 3$ lines of H¹³CO⁺, HN¹³C, and H¹³CN, all the molecular transitions were observed with the IRAM (Instituto de Radioastronomía Milimétrica) 30 m telescope at Pico Veleta (Spain). We used the wobbler-switched and frequency-switched modes with position and frequency throws of 240" and 7.2 MHz, respectively. The beam sizes were $\sim 28''$, 19", and 11" at ~ 90 , 130, and 260 GHz, respectively. The SIS receivers were tuned to a single sideband with rejections of ≥ 10 dB. We used the spectrometers of VESPA (VErsatile SPectrometer Array) with a spectral resolution of 40 kHz, i.e., with velocity resolutions of ~ 0.14 , 0.09, and 0.05 km s⁻¹ at ~ 90 , 130, and 260 GHz, respectively. Typical system temperatures ranged from 100 to 500 K.

The $J = 4 \rightarrow 3$ lines (~ 347 GHz) of H¹³CO⁺, HN¹³C, and H¹³CN were observed with the James Clerk Maxwell Telescope (JCMT) at Mauna Kea (Hawaii) in the frequency-switched mode with a frequency throw of 16 MHz. The beam size was $\sim 14''$, which matches the IRAM 30 m beam for the $J = 3 \rightarrow 2$ lines of H¹³CO⁺ and HN¹³C. We used the B3 receiver in the dual-mixer and single-sideband modes with an image rejection of 12–14 dB. The Digital Autocorrelation Spectrometer (DAS) provided a spectral resolution of 156 kHz (~ 0.14 km s⁻¹). The system temperatures were of 450–560 K. All the intensities

¹ Departamento de Astrofísica Molecular e Infrarroja, Instituto de Estructura de la Materia, CSIC, C/Serrano 121, E-28006 Madrid, Spain; izaskun@damir.iem.csic.es, martin@damir.iem.csic.es, arturo@damir.iem.csic.es.

² Department of Physics and Astronomy, University College London, London WC1E 6BT, England, UK; sv@star.ucl.ac.uk, j.tennyson@ucl.ac.uk.

³ Instituto de Radioastronomía Milimétrica, Avda. Divina Pastora, Local 20, E-18012 Granada, Spain; martin@iram.es.

⁴ Escuela Universitaria de Óptica, Departamento de Matemática Aplicada (Biomatemática), Universidad Complutense de Madrid, Avda. Arcos de Jalón s/n, E-28037 Madrid, Spain.

⁵ Laboratoire d'Astrophysique, Observatoire de Grenoble, BP 53, 38041 Grenoble Cedex 09, France; Alexandre.Faure@obs.ujf-grenoble.fr.

⁶ These excitation differences between ion and neutral molecules reflect a fundamental difference between the corresponding electron-impact cross sections at low energy: for neutrals, cross sections go to zero at the threshold; for ions, they are large and finite (e.g., Chu & Dalgarno 1974).

were calibrated in units of antenna temperature and converted to main-beam temperatures using efficiencies of 0.82, 0.74, and 0.52 at ~ 90 , 130, and 260 GHz for the IRAM 30 m data, respectively, and 0.63 for the JCMT data.

Figure 1 shows the line profiles of all transitions measured toward L1448-mm (0, 0), (0, -10), and (0, -20), and Table 1 gives the observed parameters for the different velocity components. As expected for a shock tracer in the precursor (Jiménez-Serra et al. 2004), the narrow (~ 0.6 km s $^{-1}$) SiO $J = 2 \rightarrow 1$ and $3 \rightarrow 2$ lines have single-peaked profiles whose peak emission is slightly redshifted (~ 5.2 km s $^{-1}$; Fig. 1) with respect to the ambient 4.7 km s $^{-1}$ cloud. The $J = 1 \rightarrow 0$ lines of H^{13}CO^+ , HN^{13}C , and H^{13}CN show double-Gaussian profiles (the ambient and shock precursor components) and have line widths of ~ 0.6 – 0.7 km s $^{-1}$ for each of the velocity components. The H^{13}CO^+ emission peaks at the shock precursor component toward the positions where narrow SiO is detected (Jiménez-Serra et al. 2004). However, the HN^{13}C peak emission is centered at the ambient cloud in L1448-mm (0, 0). Toward L1448-mm (0, -10) and (0, -20), the HN^{13}C emission is progressively redshifted to 5.4 and 5.6 km s $^{-1}$, respectively (see vertical dotted lines in Fig. 1). H^{13}CO^+ and H^{13}CN also peak at 5.4 and 5.6 km s $^{-1}$ toward these positions, as if we were observing the evolutionary effects of the propagation of C-type shocks through the unperturbed gas. The detection of broad SiO emission (terminal velocity of ~ 25 km s $^{-1}$) toward L1448-mm (0, -10) and (0, -20) supports this idea.

The $J = 3 \rightarrow 2$ and $4 \rightarrow 3$ lines of H^{13}CO^+ , HN^{13}C , and H^{13}CN tend to be single-peaked and have line widths of ~ 0.7 km s $^{-1}$ (Table 1). The HN^{13}C emission arising from the ambient gas toward L1448-mm (0, 0) is weak. However, the high- J H^{13}CO^+ emission measured toward L1448-mm (0, 0) and (0, -10) is very bright and mainly arises from the precursor component. H^{13}CO^+ also shows faint emission centered at the ambient cloud toward L1448-mm (0, 0). The SiO $J = 5 \rightarrow 4$ and H^{13}CN $J = 4 \rightarrow 3$ lines have not been detected in any of the velocity components toward L1448-mm.

3. EXCITATION DIFFERENCES BETWEEN ION AND NEUTRAL MOLECULAR SPECIES

A first look at the high- J lines of H^{13}CO^+ , HN^{13}C , and H^{13}CN clearly shows that the emission of H^{13}CO^+ is anomalously bright in the shock precursor component compared to that of the neutrals. Since the emission of all these species is expected to be optically thin, the line intensity ratio between different transitions is directly related to the excitation temperature of the ion and neutral fluids in the ambient and shock precursor gas. The integrated line ratios between the $J = 3 \rightarrow 2$ and $1 \rightarrow 0$ lines for H^{13}CO^+ and HN^{13}C , and between the $J = 4 \rightarrow 3$ and $1 \rightarrow 0$ lines for H^{13}CO^+ and H^{13}CN , in the ambient and precursor components are shown in Table 2. In the ambient cloud, the line ratios of H^{13}CO^+ are very similar to those of HN^{13}C and H^{13}CN . However, the line intensity ratios of H^{13}CO^+ in the precursor component are up to a factor of 9 larger than those of the neutrals, indicating a higher excitation for the ions in this component. H^{13}CO^+ is “selectively” excited in the precursor gas.

We can estimate the H_2 densities required to explain the line intensity ratios of Table 2 by using a model for the excitation of the observed molecules. Let us consider the large velocity gradient (LVG) approximation and the only excitation by H_2 collisions. We have used the H_2 collisional rates of Turner et al. (1992) for SiO, Flower (1999) for H^{13}CO^+ , and Green & Thaddeus (1974) for HN^{13}C and H^{13}CN . Considering that the emissions of all molecules have similar spatial distributions,

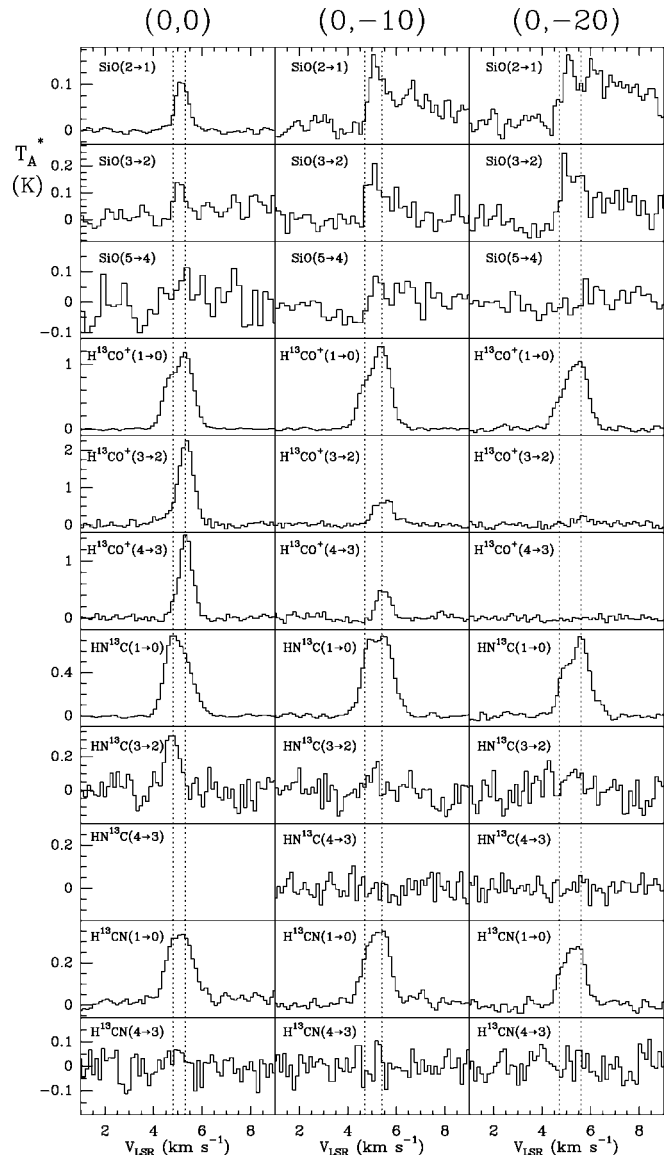


FIG. 1.—Low- and high- J lines of SiO, H^{13}CO^+ , HN^{13}C , and H^{13}CN observed toward L1448-mm. Offsets in arcseconds are shown in the upper part of the columns ($\alpha_{J2000} = 03^{\text{h}}25^{\text{m}}38^{\text{s}}.0$, $\delta_{J2000} = 30^{\circ}44'05''$). The vertical dotted lines show the ambient gas at 4.7 km s $^{-1}$ and the precursor component at 5.2 km s $^{-1}$ toward L1448-mm (0, 0), and at 5.4 and 5.6 km s $^{-1}$ toward L1448-mm (0, -10) and (0, -20), respectively.

and a kinetic temperature of 21 K (see Curiel et al. 1999), the estimated H_2 densities and molecular column densities are shown in Table 3. For the ambient gas, the derived H_2 densities for all molecules are of few $\times 10^5$ cm $^{-3}$, consistent with excitation by H_2 collisions. The H_2 densities derived from SiO, HN^{13}C , and H^{13}CN in the precursor are similar to those of the ambient gas. However, as expected from the large H^{13}CO^+ line ratios, the H_2 densities required for this ion in the precursor gas are a factor of ≥ 10 larger than the H_2 densities derived from the neutral species (Table 3). This clearly illustrates that excitation only by H_2 collisions with a single density cannot explain the excitation of H^{13}CO^+ in the precursor.

4. COLLISIONAL EXCITATION BY ELECTRONS

Since the ions have been selectively excited in the precursor component by an extra mechanism besides the H_2 impact, we explore the possibility that this selective excitation is produced

TABLE 1
OBSERVED PARAMETERS OF THE SiO, H¹³CO⁺, HN¹³C, AND H¹³CN LINES

LINE	(0, 0)			(0, -10)			(0, -20)		
	V _{LSR} (km s ⁻¹)	Δ <i>v</i> (km s ⁻¹)	T _A [*] (K)	V _{LSR} (km s ⁻¹)	Δ <i>v</i> (km s ⁻¹)	T _A [*] (K)	V _{LSR} (km s ⁻¹)	Δ <i>v</i> (km s ⁻¹)	T _A [*] (K)
SiO (2 → 1)	~4.7	...	≤0.012 ^a	~4.7	...	≤0.048	~4.7	...	≤0.060
	5.170(8)	0.62(2)	0.107(5)	5.18(3)	0.60(8)	0.11(2)	5.11(2)	0.41(8)	0.10(2)
SiO (3 → 2)	~4.7	...	≤0.084	~4.7	...	≤0.132	~4.7	...	≤0.183
	5.08(7)	0.6(2)	0.14(1)	5.02(6)	0.5(1)	0.17(3)	5.20(7)	0.9(1)	0.18(4)
SiO (5 → 4)	~4.7	...	≤0.171	~4.7	...	≤0.130	~4.7	...	≤0.084
	~5.2	...	≤0.171	~5.2	...	≤0.130	~5.2	...	≤0.084
H ¹³ CO ⁺ (1 → 0)	4.584(7)	0.59(1)	0.629(8)	4.685(6)	0.70(1)	0.62(2)	4.84(2)	0.84(5)	0.46(3)
	5.300(5)	0.81(1)	1.160(8)	5.424(0)	0.796(8)	1.26(2)	5.545(9)	0.84(2)	1.00(3)
H ¹³ CO ⁺ (3 → 2)	4.7(0)	0.6(0)	0.28(8)	~4.7	...	≤0.168	~4.7	...	≤0.225
	5.356(6)	0.69(2)	2.25(8)	5.48(2)	0.95(5)	0.66(8)	5.72(7)	0.6(2)	0.24(4)
H ¹³ CO ⁺ (4 → 3)	4.7(0)	0.55(0)	0.08(5)	~4.7	...	≤0.162	~4.7	...	≤0.138
	5.338(7)	0.62(2)	1.43(5)	5.47(2)	0.63(4)	0.52(4)	~5.2	...	≤0.138
HN ¹³ C (1 → 0)	4.785(3)	0.806(7)	0.72(1)	4.81(2)	0.65(2)	0.56(2)	4.85(2)	0.50(4)	0.34(3)
	5.468(6)	0.78(2)	0.36(1)	5.53(2)	0.88(3)	0.71(2)	5.59(1)	0.86(4)	0.68(3)
HN ¹³ C (3 → 2)	4.75(5)	0.6(1)	0.35(4)	~4.7	...	≤0.261	~4.7	...	≤0.264
	~5.2	...	≤0.237	~5.2	...	≤0.261	~5.2	...	≤0.264
HN ¹³ C (4 → 3)	~4.7	...	≤0.117	~4.7	...	≤0.108
	~5.2	...	≤0.117	~5.2	...	≤0.108
H ¹³ CN (1 → 0)	4.86(5)	1.06(7)	0.18(2)	4.89(2)	0.80(6)	0.27(1)	4.9(1)	0.6(2)	0.16(1)
	5.32(2)	1.25(4)	0.21(2)	5.52(2)	0.70(6)	0.30(1)	5.5(1)	0.7(2)	0.28(1)
H ¹³ CN (4 → 3)	~4.7	...	≤0.141	~4.7	...	≤0.138	~4.7	...	≤0.141
	~5.2	...	≤0.141	~5.2	...	≤0.138	~5.2	...	≤0.141

^a The upper limits of the line intensities correspond to the 3 σ noise level in the spectra.

by collisions with electrons. The efficiency of excitation of molecular ions by electrons can be significantly larger than that of neutral molecules at the low temperatures of dark clouds. To illustrate this, we compare the electron collisional rates of HCO⁺ and HCN for the $J = 0 \rightarrow 1$ and $1 \rightarrow 2$ transitions at low and high temperatures. While the HCO⁺/HCN collisional coefficient ratio is only ~ 1.6 at 100 K, this ratio is increased to ~ 6 at a temperature of 10 K (Bhattacharyya et al. 1981; Saha et al. 1981). This difference between the HCO⁺ and HCN rates is expected to further increase for higher initial J and large ΔJ transitions (Bhattacharyya et al. 1981). New calculations of the HCO⁺ and H¹³CO⁺ collisional rates for all transitions between $J = 1$ and $J = 5$ (A. Faure & J. Tennyson 2006, in preparation), show that the HCO⁺ rates with $\Delta J \geq 2$, exceed those of HCN by more than 1 order of magnitude at 10 K. This naturally introduces a differential excitation between the ions and neutrals as observed in the precursor component.

We can constrain the electron density required to reproduce the H¹³CO⁺ line intensities observed in the precursor component by using the LVG model, including collisions with both H₂ and electrons. For an H₂ density of $\sim 3 \times 10^5$ cm⁻³ (similar to that derived from HN¹³C and H¹³CN; Table 3) and a temperature of 21 K, the estimated electron densities in the precursor component toward L1448-mm (0, 0) and (0, -10) in the optically thin case [$N(\text{H}^{13}\text{CO}^+) \sim 10^{11}$ cm⁻²] are ~ 240 and 600 cm⁻³, respectively, which correspond to fractional ionizations of 8×10^{-4} and 2×10^{-3} . However, in the optically thick case [$N(\text{H}^{13}\text{CO}^+) \sim (7-9) \times 10^{12}$ cm⁻²], and for higher

temperatures ($\sim 35-45$ K), the fractional ionization in the precursor decreases to $\sim 5 \times 10^{-5}$. Although even higher temperatures (~ 100 K) could reproduce the H¹³CO⁺ intensities in the precursor component for a fractional ionization of $\leq 10^{-7}$, the derived HN¹³C and H¹³CN line intensities would clearly exceed (by up to a factor of 5) the upper limits of Table 1. The derived ionization fraction implies an electron density enhancement by a factor of ~ 500 with respect to that of the quiescent gas ($\leq 10^{-7}$).

Considering an extrapolation of the electron collisional rates of Saha et al. (1981) for HCN, we can now estimate the expected line intensities of HN¹³C and H¹³CN in the precursor for the fractional ionization ($\sim 5 \times 10^{-5}$) derived from H¹³CO⁺. The expected intensities are similar to those reported in Table 1, except for the HN¹³C $J = 3 \rightarrow 2$ line whose predicted intensity

TABLE 3
DERIVED H₂ DENSITIES AND COLUMN DENSITIES FOR SiO, H¹³CO⁺, HN¹³C, AND H¹³CN

MOLECULE	H ₂ DENSITY (cm ⁻³)		COLUMN DENSITY (cm ⁻²)	
	Ambient	Precursor	Ambient	Precursor
(0, 0)				
H ¹³ CO ⁺	1.3×10^5	2.0×10^6	6.7×10^{11}	2.2×10^{12}
SiO	2.7×10^5	...	1.4×10^{11}
HN ¹³ C	1.9×10^5	$\leq 3.4 \times 10^{5a}$	1.4×10^{12}	5.1×10^{11}
H ¹³ CN	$\leq 1.8 \times 10^6$	$\leq 1.6 \times 10^6$	2.1×10^{11}	2.4×10^{11}
(0, -10)				
H ¹³ CO ⁺	$\leq 1.3 \times 10^5$	6.0×10^6	4.2×10^{11}	1.8×10^{12}
SiO	4.0×10^5	...	1.3×10^{11}
HN ¹³ C	$\leq 1.9 \times 10^5$	$\leq 1.1 \times 10^5$	1.1×10^{12}	1.9×10^{12}
H ¹³ CN	$\leq 1.3 \times 10^6$	$\leq 1.2 \times 10^6$	3.0×10^{11}	3.4×10^{11}
(0, -20)				
H ¹³ CO ⁺	$\leq 1.6 \times 10^5$	$\leq 5.7 \times 10^4$	3.1×10^{11}	1.0×10^{12}
SiO	5.9×10^5	...	1.3×10^{11}
HN ¹³ C	$\leq 4.0 \times 10^5$	$\leq 1.3 \times 10^5$	4.5×10^{11}	1.6×10^{12}
H ¹³ CN	$\leq 2.0 \times 10^6$	$\leq 1.2 \times 10^6$	1.9×10^{11}	3.2×10^{11}

^a The upper limits to the H₂ densities were estimated from the 3 σ level.

TABLE 2
INTEGRATED LINE INTENSITY RATIOS

RATIO	MOLECULE	(0, 0)		(0, -10)	
		Ambient	Precursor	Ambient	Precursor
(3 → 2/1 → 0)	H ¹³ CO ⁺	0.5	1.6	≤0.1	0.6
	HN ¹³ C	0.4	≤0.2	≤0.2	≤0.1
(4 → 3/1 → 0)	H ¹³ CO ⁺	0.1	0.9	≤0.1	0.3
	H ¹³ CN	≤0.2	≤0.1	≤0.2	≤0.2

exceeds the upper limits in Table 1 by a factor of ~ 2 . Given the uncertainties in the rates, and the relative spatial distribution of the ion and neutral gas, we find that the data are consistent with the idea of an electron density enhancement in the precursor component. High angular resolution observations are required to establish the spatial distribution of the ion and neutral species in the precursor.

5. ON THE ORIGIN OF THE ELECTRON DENSITY ENHANCEMENT

Toward the quiescent gas of L1448-mm, the ion and neutral fluids show similar excitation conditions. In fact, the H_2 densities obtained from the ions and neutrals are all consistent with $\text{few} \times 10^5 \text{ cm}^{-3}$ for this component. Since the fractional ionization is expected to be of $\leq 10^{-7}$ in the ambient cloud (Guélin et al. 1982; Caselli et al. 1998), the high- J $H^{13}CO^+$ and $HN^{13}C$ excitation in this component is completely dominated by H_2 collisions.

In contrast to the quiescent gas, the precursor component shows an overexcitation in $H^{13}CO^+$. The line ratios and H_2 densities estimated for this ion in the precursor gas are a factor of 10 larger than those for SiO, $HN^{13}C$, and $H^{13}CN$. In § 4, we have shown that an electron density enhancement by a factor of ~ 500 in this component could explain the overexcitation in $H^{13}CO^+$. Modeling of C-type shocks shows that the UV fluorescence radiation generated by the collisional excitation of H_2 in the magnetic precursor rapidly enhances the ion and electron densities in this region ($t \leq 100$ yr from the inception of the C-type shock; Flower et al. 1996; Flower & Pineau des Forêts 2003). One may think that the probability of detecting this enhancement toward molecular outflows for such short time-scales is negligible. However, L1448-mm is a very young outflow ($t_{\text{dyn}} \sim 1000$ yr), and the dynamical timescales derived from the proper motions of the SiO bullets (~ 90 yr; Girart & Acord 2001) are consistent with the possibility of detecting the shock precursor as predicted by C-type shock models. In fact, the more redshifted velocities toward L1448-mm (0, -10) and (0, -20) are consistent with the observation of different evolutionary stages of C-type shocks in different positions in the outflow as predicted by models.

We can use our results to constrain the electron density enhancement produced by the precursor. For optically thin emis-

sion and low temperatures, the derived fractional ionization is $\sim 10^{-3}$. Flower et al. (1996) and Flower & Pineau des Forêts (2003) predicted that the ionization fraction is increased to $\sim 10^{-5}$ in the precursor stage. Our estimate of the fractional ionization clearly exceeds these results by a factor of 100 and even exceeds the cosmic abundance of atomic carbon (the main repository of positive charge in dark clouds; $\chi(C) \sim (2-3) \times 10^{-4}$; Cardelli et al. 1996) by a factor of ~ 5 . However, if we increase the kinetic temperature (ions are expected to be rapidly heated by the precursor; Draine 1980) and consider optically thick emission, the ionization fraction can be decreased to $\sim 5 \times 10^{-5}$. This result is consistent with the model predictions (Flower et al. 1996; Flower & Pineau des Forêts 2003).

We cannot rule out the possibility that the ion and electron enhancement in the precursor component is produced by the radiative precursor of J-type shocks (Shull & McKee 1979). Chemical models that include illumination by UV photons predict the enhancement of molecules such as HCO^+ , HCO, and HCN for $t \leq 300$ yr (Viti & Williams 1999; Viti et al. 2003). However, HCO (a typical photon-dominated region tracer; Schenewerk et al. 1988) is not detected in the precursor component (Jiménez-Serra et al. 2004), which suggests that the ion and electron enhancements are likely due to the magnetic precursor of C-type shocks.

In summary, the differences in the kinematics and excitation between the ion and neutral components in the L1448-mm molecular outflow are clear indicators of the early interaction of C-type shocks with the ambient gas. The overexcitation in $H^{13}CO^+$ has allowed us to measure, for the first time, the electron density enhancement in the precursor of a C-type shock. The estimated fractional ionization in the precursor component is of $\sim 5 \times 10^{-5}$, which implies an enhancement of the electron densities by a factor of ≥ 500 with respect to the ambient gas.

We acknowledge the Spanish MEC for the support provided by projects AYA2002-10113-E, AYA2003-02785-E, and ESP2004-00665 and by the ‘‘Comunidad de Madrid’’ Government under PRICIT project S-0505/ESP-0237 (ASTROCAM). This work has benefited from research funding from the European Community’s Sixth Framework Programme.

Facilities: JCMT, IRAM 30 m.

REFERENCES

- Bhattacharyya, S. S., Bhattacharyya, B., & Narayan, M. V. 1981, *ApJ*, 247, 936
 Cardelli, J. A., Meyer, D. M., Jura, M., & Savage, B. D. 1996, *ApJ*, 467, 334
 Caselli, P., Walmsley, C. M., Terzieva, R., & Herbst, E. 1998, *ApJ*, 499, 234
 Chu, S.-I., & Dalgarno, A. 1974, *Phys. Rev. A*, 10, 788
 Curiel, S., Torrelles, J. M., Rodríguez, L. F., Gómez, J. F., & Anglada, G. 1999, *ApJ*, 527, 310
 Draine, B. T. 1980, *ApJ*, 241, 1021
 Faure, A., & Tennyson, J. 2001, *MNRAS*, 325, 443
 Flower, D. R. 1999, *MNRAS*, 305, 651
 Flower, D. R., & Pineau des Forêts, G. 2003, *MNRAS*, 343, 390
 Flower, D. R., Pineau des Forêts, G., Field, D., & May, P. W. 1996, *MNRAS*, 280, 447
 Girart, J. M., & Acord, J. M. P. 2001, *ApJ*, 552, L63
 Green, S., & Thaddeus, P. 1974, *ApJ*, 191, 653
 Guélin, M., Langer, W. D., & Wilson, R. W. 1982, *A&A*, 107, 107
 Jiménez-Serra, I., Martín-Pintado, J., Rodríguez-Franco, A., & Marcelino, N. 2004, *ApJ*, 603, L49
 Langer, W. D. 1985, in *Protostars and Planets II*, ed. D. C. Black & M. S. Matthews (Tucson: Univ. Arizona Press), 650
 Saha, S., Ray, S., Bhattacharyya, B., & Barua, A. K. 1981, *Phys. Rev. A*, 23, 2926
 Schenewerk, M. S., Snyder, L. E., Hollis, J. M., Jewell, P. R., & Ziurys, L. M. 1988, *ApJ*, 328, 785
 Shull, J. M., & McKee, C. F. 1979, *ApJ*, 227, 131
 Turner, B. E., Chan, K.-W., Green, S., & Lubowich, D. A. 1992, *ApJ*, 399, 114
 Viti, S., Girart, J. M., Garrod, R., Williams, D. A., & Estalella, R. 2003, *A&A*, 399, 187
 Viti, S., & Williams, D. A. 1999, *MNRAS*, 310, 517